RESEARCH PAPERS

Acta Cryst. (1994). A**50**, 553–566

Classification of Local Configurations in Quasicrystals

BY M. BAAKE

Institut für Theoretische Physik, Universität Tübingen, Auf der Morgenstelle 14, *D*-72076 *Tübingen, Germany*

S. I. BEN-ABRAHAM

Department of Physics, Ben-Gurion University, POB 653, *IL*-84105 *Beer-Sheba, Israel*

AND R. KLITZING, P. KRAMER AND M. SCHLOTTMAN

Institut für Theoretische Physik, Universität Tübingen, Auf der Morgenstelle 14, *D*-72076 *Tübingen, Germany*

(*Received* 23 *September* 1993; *accepted* 7 *February* 1994)

Abstract

Aperiodic crystalline structures, commonly called quasicrystals, display a great variety of combinatorially possible local configurations. The local configurations of first order are the vertex configurations. This paper investigates, catalogues and classifies in detail the latter in the following important two-dimensional cases: the Penrose tiling, the decagonal triangle tiling and some twelvefold tilings, including the patterns of Stampfli, Gähler, Niizeki and Socolar, as well as the square-triangle and the shield patterns. The main result is a comprehensive study of the three-dimensional primitive icosahedral tiling in its random version. All its 10 527 combinatorially possible noncongruent vertex configurations are constructed, coded, listed and classified. Methods for coding and representation of local configurations by formulae and diagrams, in particular those of Schlegel, are discussed. The paper also describes the algorithm used to generate them. The formal classification of local configurations by the characteristic integers rank, degree and order is also discussed.

1. Introduction

Local configurations in random tilings should be of interest to quasicrystallographers, as well as to crystallographers and quasicrystallographers. In this *Introduction*, we try to give some convincing arguments in favour of this statement and we attempt to support them by the content of this paper.

Almost a decade ago, Shechtman, Blech, Gratias & Cahn (1984) and almost simultaneously Ishimasa, Nissen & Fukano (1984) discovered, recognized and announced the existence of novel aperiodic crystalline phases in the Al-Mn and Cr-Ni systems, respectively. These were promptly and for very good reasons dubbed quasicrystals (Levine & Steinhardt, 1984).

Since then, a plethora of quasicrystalline systems has been found (Jarić, 1990; Nissen & Beeli, 1990; DiVicenzo & Steinhardt, 1991; Bancel, 1991). The microscopic structure of these phases has ever since been a subject of intensive and extensive research, both experimental and theoretical. Various structural models have been suggested in different instances and by different authors. The models fall roughly into three classes: (1) the quasiperiodic tiling model (Kramer & Neri, 1984; Levine & Steinhardt, 1984; Duneau & Katz, 1985; DiVicenzo & Steinhardt, 1991; Katz & Duneau, 1986; Socolar & Steinhardt, 1986); (2) the orientationally ordered polyhedral glass model (Jarić, 1990; Nissen & Beeli, 1990), commonly and imprecisely called the 'icosahedral glass' model; (3) the random tiling model (Elser, 1985; Widom, Strandburg & Swendsen, 1987; Jarić, 1990; Henley, 1990, 1991; Nissen & Beeli, 1990; Tang, 1990; Bancel, 1991; DiVicenzo & Steinhardt, 1991).

It seems that phases with the primitive icosahedral structure, represented by Al-Cu-Li, may be adequately described by the random tiling model, whereas the face-centred icosahedral phases, represented by Al-Cu-Fe, are apparently fairly good realizations of a quasiperiodic tiling. Important evidence for the relevance of quasiperiodic tiling models for the octagonal, decagonal and dodecagonal phases comes from high-resolution transmission electron microscopy (Nissen & Beeli, 1990, 1993; Hiraga, 1991), X-ray diffraction (Steurer & Kuo, 1990) and scanning tunnelling microscopy (Kortan, Becker, Thiel & Chen, 1990; Becker & Kortan, 1991).

The wealth of known quasicrystalline phases and those yet to be discovered opened up a new and immensely rich world of aperiodic ordered solids. We

must expect to find an extremely wide, intricate and fairly dense spectrum of ordering in this realm. One of its unifying features is the established physical reality of symmetries forbidden by the dogma of classical crystallography in spite of past and present attempts to explain away experimental evidence (Hardy & Silcock, 1955/56; Sastry, Suryanarayana, Van Sande & Van Tendeloo, 1978; Pauling, 1985). In order to understand these aperiodic phases, we usually surmise the existence of some ideal underlying structure and try to investigate the deviations therefrom. This is one avenue leading to the study of defective local configurations.

From a quite different but by no means contradictory point of view, we assume only the existence of a few building blocks and try to assemble them in every possible way. Thus, we are again led to the study of all combinatorially possible local configurations. In this approach, there are no defective configurations. Rather, every possible local configuration is part of the global structure. Since there is no obvious limitation to the symmetry of the building blocks, the resulting structure is expected to inherit at least some features of this symmetry. For the study of aperiodic ordered structures, the investigation, cataloguing and classification of local configurations should be of interest.

In § 2, we explain our intentions using as example the well known Penrose tiling. §§ 3 and 4 deal with instances of planar tilings, in particular the decagonal triangle tiling and some twelvefold tilings. [The octagonal case is left for diligent readers as an easy exercise. They may check their result for one interesting example, the Ammann–Beenker tiling, with the published literature (Baake & Joseph, 1990).] § 5 is the core of this paper. It is devoted to the three-dimensional primitive icosahedral tiling. § 6 clarifies our methods of coding and representation of local configurations while § 7 explains the algorithm used to generate them. § 8 deals with the formal classification of local configurations. Some minor technical topics are deferred to the Appendix to avoid distraction.

2. The random rhombic Penrose tiling

We start with the random rhombic Penrose tiling. This well known example will serve as a warm-up exercise, as well as a paradigm of things to come.

The tiles are the two bare (*i.e.* undecorated) Penrose rhombi with equal sides a: a large (or thick or fat) kind L with acute angle $2\pi/5$ and a small (or thin or skinny) kind S with acute angle $\pi/5$. We construct all combinatorially possible local configurations of order 1, in other words, all vertex configurations. That amounts to partitioning the full plane angle around a node into integer multiples of an angle unit ω, determined by the point symmetry of the tiling. In other words, we perform an ordered partition of a natural number, the *count* s, into a set of given natural numbers $\mathcal{S} = \{s_1, \ldots, s_k\}$, sometimes subject to certain obvious constraints. The numbers s_i are the internal angles of the tiles in units of ω, so they are convenient labels for the possible corners. It is expedient to list the numbers s_i in descending order, that is, to have $s_i \geq s_j$ if $i < j$.

In our case, $\omega = \pi/5$, $s = 10$, $k = 4$, and $\mathcal{S} = \{4,3,2,1\}$. First, we perform the partition without ordering; thus we get k-tuples of integers $\sigma = \{\sigma_1, \ldots, \sigma_k\}$, satisfying

$$s = \sum_{i=1}^{k} \sigma_i s_i, \qquad \sigma_i \in \mathbb{N}_0.$$

The vertices are classified by the k-tuples σ into classes of the same summary *composition*, $n_1^{\sigma_1} \ldots n_k^{\sigma_k}$, a term borrowed from chemistry. In the present instance, we have

$$\boxed{10} = 2 \times \boxed{4} + 0 \times \boxed{3} + 1 \times \boxed{2} + 0 \times \boxed{1}$$
$$= \ldots \textit{ etc.},$$

whence we get the composition formulae $4^2 2$, ... *etc.* Sometimes it is more expedient to write out the k-tuples σ themselves, {2,0,1,0}, ... *etc.*

Next, we permute the elements within the composition classes with repetition and without a fixed starting point. Thus, we gain all *isomers* of the same composition. The result is a complete list of all vertex configurations of the given tiling. For the random rhombic Penrose tiling, it is shown in Fig. 1 and listed in Table 1.

Each configuration has a multiplicity, *i.e.* it may occur within the pattern in a number of different orientations, determined by the fundamental symmetry of the tiling. Some of these orientations may be indistinguishable. The vertex list includes the symmetry and multiplicity of the vertices (*cf.* Table 1). In particular, some vertices have mirror symmetry, while others do not. The latter, in chemical parlance, show *enantiomorphy*, *i.e.* have different left and right enantiomers. In our example, we have, up to rotations, 75 vertex configurations. Among these, there are 21 enantiomorphic pairs. Thus, ignoring rotations and reflections, we are left with 54 configurations.

Out of these vertex configurations, only 16 occur in the class of perfect generalized Penrose tilings although never do all 16 appear in one single tiling. Only a single one of these, the 'cocktail', has different enantiomers. We are naturally led to classify all possible configurations with respect to their deviation from the perfect tiling. This is done by means of two characteristic integers: *degree* and *rank* (Ben-Abraham, Baake, Kramer & Schlottmann, 1993). The degree g is the maximum dimension of a facet shared by such subconfigurations that cannot occur in the ideal tiling. For completeness, the degree of a regular vertex configuration is defined as

-1. The rank r is the dimension of the dual overlap if it exists. If it does not exist, the configuration is *strictly forbidden* or *prohibited* and is assigned a rank of -1. The degree g of the random rhombic Penrose tiling vertices is also listed in Table 1.

We come now to the question of representing the vertex configurations. Of course, the most intuitive way to represent them is to depict them explicitly, as is done in Fig. 1. One may save some space and effort by showing only the links emanating from the vertex node. However, it is clear that such a representation is rather wasteful of space, time and effort and that it becomes awkward in three dimensions and impossible in even higher dimensions. Moreover, the pictorial representation is hardly suited for data processing. Therefore, some reasonable coding is necessary.

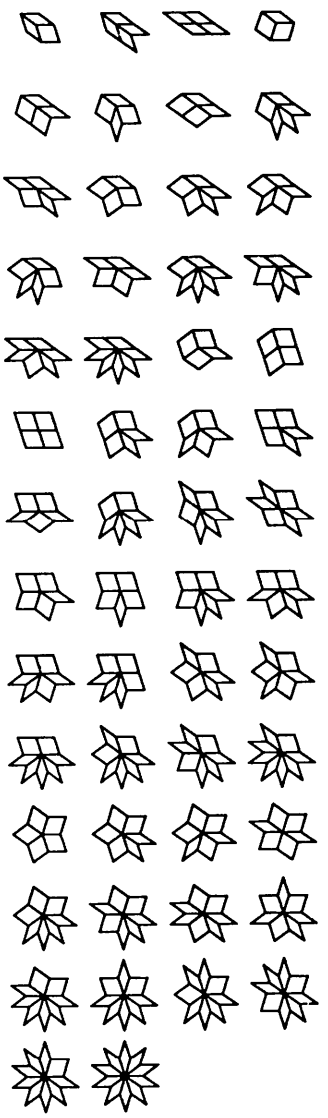

Fig. 1. Vertex configurations of the random rhombic Penrose tiling.

Table 1. *Vertex configurations of the random rhombic Penrose tiling*

For the multiplicities, we have given orientations and enantiomorphies separately. The configurations marked with an asterisk occur also as *regular* configurations within the class of perfect, *generalized* Penrose tilings.

Partition	#	Formula	Symmetry H-M	Symmetry Sch	Multiplicity	Deg g
{2,0,1,0}	1	$4^2 2$	m	C_s	10·1	−1
{2,0,0,2}	2	$4^2 1^2$	m	C_s	10·1	1
	3	4141	$mm2$	C_{2v}	5·1	1
{1,2,0,0}	4	43^2	m	C_s	10·1	−1
{1,1,1,1}	5	4321	1	C_1	10·2	1
	6	4312	1	C_1	10·2	0*
	7	4231	1	C_1	10·2	1
{1,1,0,3}	8	431^3	1	C_1	10·2	1
	9	4131^2	1	C_1	10·2	1
{1,0,3,0}	10	42^3	m	C_s	10·1	−1
{1,0,2,2}	11	$42^2 1^2$	1	C_1	10·2	1
	12	42121	1	C_1	10·2	1
	13	$421^2 2$	m	C_s	10·1	0*
	14	$412^2 1$	m	C_s	10·1	1
{1,0,1,4}	15	421^4	1	C_1	10·2	1
	16	4121^3	1	C_1	10·2	1
	17	$41^2 21^2$	m	C_s	10·1	1
{1,0,0,6}	18	41^6	m	C_s	10·1	1
{0,3,0,1}	19	$3^3 1$	m	C_s	10·1	0*
{0,2,2,0}	20	$3^2 2^2$	m	C_s	10·1	1
	21	3232	$mm2$	C_{2v}	5·1	1
{0,2,1,2}	22	$3^2 21^2$	1	C_1	10·2	1
	23	$3^2 121$	m	C_s	10·1	−1
	24	3231^2	m	C_s	10·1	1
	25	32131	1	C_1	10·2	1
{0,2,0,4}	26	$3^2 1^4$	m	C_s	10·1	0
	27	3131^3	m	C_s	10·1	0
	28	$31^2 31^2$	$mm2$	C_{2v}	5·1	0
{0,1,3,1}	29	$32^3 1$	1	C_1	10·2	1
	30	$32^2 12$	1	C_1	10·2	1
{0,1,2,3}	31	$32^2 1^3$	1	C_1	10·2	1
	32	32121^2	1	C_1	10·2	1
	33	$321^2 21$	1	C_1	10·2	1
	34	$321^3 2$	m	C_s	10·1	1
	35	$312^2 1^2$	1	C_1	10·2	0
	36	312121	m	C_s	10·1	0*
{0,1,1,5}	37	321^5	1	C_1	10·2	1
	38	3121^4	1	C_1	10·2	0
	39	$31^2 21^3$	1	C_1	10·2	0
{0,1,0,7}	40	31^7	m	C_s	10·1	0
{0,0,5,0}	41	2^5	$5m$	C_{5v}	2·1	−1
{0,0,4,2}	42	$2^4 1^2$	m	C_s	10·1	−1
	43	$2^3 121$	m	C_s	10·1	0
	44	$2^2 12^2 1$	$mm2$	C_{2v}	5·1	0
{0,0,3,4}	45	$2^3 1^4$	m	C_s	10·1	0
	46	$2^2 121^3$	1	C_1	10·2	0
	47	$2^2 1^2 21^2$	m	C_s	10·1	−1
	48	212121^2	m	C_s	10·1	0*
{0,0,2,6}	49	$2^2 1^6$	m	C_s	10·1	0
	50	2121^5	m	C_s	10·1	0*
	51	$21^2 21^4$	m	C_s	10·1	0*
	52	$21^3 21^3$	$mm2$	C_{2v}	5·1	0
{0,0,1,8}	53	21^8	m	C_s	10·1	0*
{0,0,0,10}	54	1^{10}	$10mm$	C_{10v}	1·1	0*

Up to now, we have coded the vertices simply by listing the participating corners in the appropriate order, usually counterclockwise, around the node. The corners were, in turn, represented by their angle numbers s_i. We refer to this representation as the *direct code*.

The direct code is excellent in two dimensions and its caricature works well in one dimension. Even in higher dimensions, it still keeps working for the summary composition formulae but it fails to describe the isomers. Hence, we are forced to introduce a more elaborate scheme. This scheme, while being rather redundant in two dimensions, shows its power in higher dimensions by being fairly versatile and universal.

To characterize a vertex, we explicitly list its links in terms of the relevant star vectors $\pm \mathbf{e}_h$, for which we usually adopt the shorthand notation $h, \bar{h}$. A tile is represented by its spanning vectors enclosed in some kind of brackets. To make the recognition easy, it is worthwhile to apply two redundant but very useful strategems. We distinguish different kinds of tiles by different kinds of brackets. Moreover, we decorate the brackets by a subscript s_i to designate explicitly the corner entering the vertex. In this coding, the order of the entries is irrelevant.

In our example, the random rhombic Penrose tiling, we have the double star $\pm \mathbf{e}_h$ ($h = 1, \ldots, 5$), abbreviated to $1, \ldots, 5, \tilde{1}, \ldots, \tilde{5}$. The fat tiles, L, are coded by square brackets [ ]; the skinny ones, S, by round brackets, *i.e.* parentheses, ( ). So, for example, the code for the left cocktail, 4213, becomes

$$(\bar{3}\bar{5})_4[\bar{5}\tilde{1}]_2(\tilde{1}4)_1[4\bar{3}]_3.$$

In this instance, the tiles happen to be conveniently listed in their correct order. But the order does not matter and in three dimensions there is, of course, no ordering at all.

3. The triangle tiling

The triangle tiling (Baake, Kramer, Schlottmann & Zeidler, 1990*a*,*b*,*c*) is a prototype for all decagonal tilings. Its tiles are the two isosceles 'golden' triangles (see Fig. 2) obtained by cutting up a regular pentagon along two of its diagonals. The dimensions are a base of length a and sides of length τa for the acute triangle *Ac*; *vice versa* for the obtuse triangle *Ob*. Here $\tau = (1 + 5^{1/2})/2$ is the golden ratio.

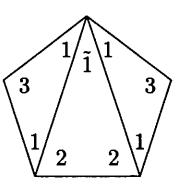

Fig. 2. The golden triangles.

Again, the count is $s = 10$ and hence the angle unit $\omega = \pi/5$. Thus, *Ac* has the corners 1,2,2, while *Ob* has corners 3,1,1. In order to distinguish the corners 1 of the two triangles, we call the top corner of the acute triangle $\tilde{1}$. Consequently, $k = 4$ and $\mathcal{S} = \{3,2,1,\tilde{1}\}$. Vertices of the tiling have to obey the constraint that the tiles meet face to face in the perfect as well as in the random pattern. There are $9 + 2 = 11$ regular vertex configurations (Fig. 3).

The random pattern has altogether $120 + 78 = 198$ such configurations. They are listed in Table 4, in the Appendix.

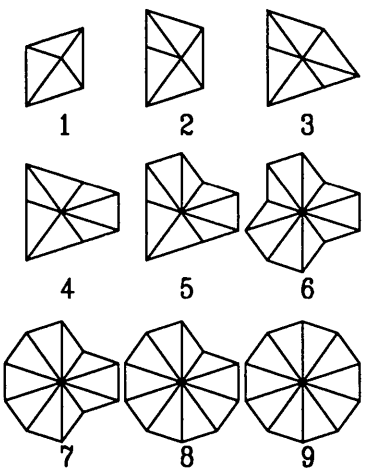

Fig. 3. The regular vertex configurations of the triangle tiling.

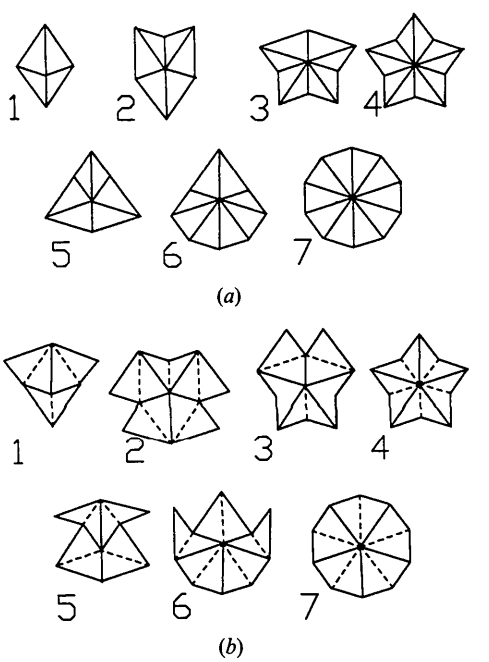

Fig. 4. The correspondence of (*a*) the Robinson vertices and (*b*) the kite-dart version of the Penrose tiling.

The same two tiles can be found in the Robinson decomposition of the Penrose tiling, also called the Robinson tiling (Robinson, 1975). This tiling is different from the triangle tiling (Baake, Schlottmann & Jarvis, 1991) but of course the random versions are the same. There are seven regular vertex configurations, all mirror symmetric (Fig. 4).

Vertex [1], the 'Simpleton' or 'Rhombus', has its node inside a decomposed Penrose rhombus of the fat kind *L*. Vertices [2] to [6] correspond to the rhombic Penrose vertices 'Pawn', 'Knight', 'North Star', 'Rook' and 'Bishop', in that order. Vertex [7], the 'Sun', arises from the three vertices 'King', 'Queen' and 'South Star'. It should be noted that the decorated rhombic Penrose tiling gives rise to three distinct Suns with different spots.

It is perhaps worthwhile to remind the reader that the Robinson vertices arise directly from the kite-dart version of the Penrose tiling by bisection of the tiles along their mirror axes. The correspondence then is as follows: [1] ace, [2] queen, [3] king, [4] star, [5] deuce, [6] jack, [7] sun [*cf.* Gardner (1977) or pages 537*ff.* of Grünbaum & Shephard (1987)].

4. The twelvefold tilings

To discuss local configurations in the twelvefold patterns, it is most expedient to start with the Stampfli pattern (Stampfli, 1990; Klitzing, 1992). The tiles are a square *Sq*, an equilateral triangle *T* and a rhombus *R*, all having sides of the same length *a*.

The count is $s = 12$, the angle unit $\omega = \pi/6$, the number of distinct corners $k = 4$ and the partition set $\mathcal{S} = \{5,3,2,1\}$. The Stampfli pattern has ten regular vertex configurations, all of them mirror symmetric (Fig. 6). Altogether, there are $116 + 63 = 179$ possible vertices. They are listed in Table 5, in the Appendix.

All patterns belonging to the same mutual local derivability class (Baake, Schlottmann & Jarvis, 1991) have, of course, related local configurations. We mention just a few.

The Gähler-Niizeki pattern (Niizeki & Mitani, 1987; Gähler, 1988) has the same three tiles, *Sq*, *T* and *R*. Hence, in its random version it has the same full vertex list as the Stampfli pattern. However, the regular vertex configurations belong to a small subset, consisting of the vertices [2] to [5] in Fig. 6.

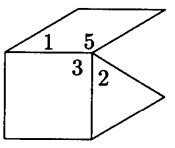

Fig. 5. The tiles of the Stampfli pattern.

The Socolar pattern (Socolar, 1989) has as tiles regular hexagons *H*, squares *Sq* and rhombi *R*, all with the same side length *a*. Thus, we have $k = 4$ and $\mathcal{S} = \{5,4,3,1\}$. The regular vertex configurations are shown in Fig. 7. The full list contains $25 + 12 = 37$ vertices. It can be recovered by taking only those random

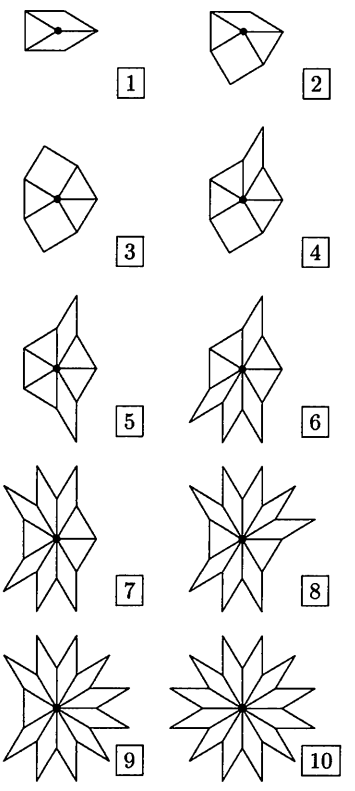

Fig. 6. The regular Stampfli vertices.

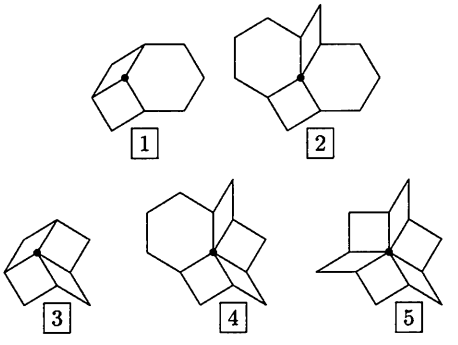

Fig. 7. The regular Socolar vertices.

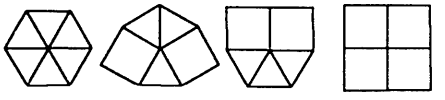

Fig. 8. The vertices of the random square-triangle tiling. Just the one consisting of squares only occurs in addition to regular ones.

Table 2. *The regular vertex configurations of the primitive icosahedral tiling*

Vert.Cf. 1	Ori.: 120		Freq.: $2/\tau^{10}$
$(\bar{2},3,4)$	$(\bar{1},\bar{4},6)$	$(\bar{1},\bar{2},5)$	$(\bar{1},3,\bar{5})$
$(2,3,6)$	$(3,4,5)$		
$[\bar{2},4,5]$	$[\bar{1},\bar{4},\bar{5}]$	$[\bar{1},\bar{2},3]$	$[\bar{1},5,6]$
$[2,\bar{4},\bar{5}]$	$[2,\bar{4},6]$	$[2,3,\bar{5}]$	$[3,5,6]$

Vert.Cf. 2	Ori.: 120		Freq.: $2/\tau^{9}$
$(\bar{2},3,4)$	$(\bar{1},\bar{4},6)$	$(\bar{1},\bar{2},5)$	$(\bar{1},3,\bar{5})$
$(2,3,\bar{4})$	$(2,3,6)$	$(3,\bar{4},\bar{5})$	$(3,4,5)$
$[\bar{2},4,5]$	$[\bar{1},\bar{4},\bar{5}]$	$[\bar{1},\bar{2},3]$	$[\bar{1},5,6]$
$[2,\bar{4},6]$	$[3,5,6]$		

Vert.Cf. 3	Ori.: 120		Freq.: $2/\tau^{13}$
$(\bar{2},3,\bar{6})$	$(\bar{2},3,4)$	$(\bar{1},\bar{4},6)$	$(\bar{1},\bar{2},5)$
$(\bar{1},3,\bar{6})$	$(\bar{1},3,\bar{5})$	$(2,3,6)$	$(3,4,5)$
$[\bar{2},4,5]$	$[\bar{1},\bar{4},\bar{5}]$	$[\bar{1},\bar{2},\bar{6}]$	$[\bar{1},5,6]$
$[2,\bar{4},\bar{5}]$	$[2,\bar{4},6]$	$[2,3,\bar{5}]$	$[3,5,6]$

Vert.Cf. 4	Ori.: 30		Freq.: $1/\tau^{12}$
$(\bar{1},\bar{4},6)$	$(\bar{1},\bar{2},5)$	$(\bar{1},3,\bar{6})$	$(\bar{1},3,\bar{5})$
$(2,3,6)$	$(3,4,5)$		
$[\bar{2},4,\bar{6}]$	$[\bar{2},4,5]$	$[\bar{1},\bar{4},\bar{5}]$	$[\bar{1},\bar{2},\bar{6}]$
$[\bar{1},5,6]$	$[2,\bar{4},\bar{5}]$	$[2,\bar{4},6]$	$[2,3,\bar{5}]$
$[3,4,\bar{6}]$	$[3,5,6]$		

Vert.Cf. 5	Ori.: 60		Freq.: $2/\tau^{12}$
$(\bar{2},3,\bar{6})$	$(\bar{2},3,4)$	$(\bar{1},\bar{4},6)$	$(\bar{1},\bar{2},5)$
$(\bar{1},3,\bar{6})$	$(\bar{1},3,\bar{5})$	$(2,3,\bar{4})$	$(2,3,6)$
$(3,\bar{4},\bar{5})$	$(3,4,5)$		
$[\bar{2},4,5]$	$[\bar{1},\bar{4},\bar{5}]$	$[\bar{1},\bar{2},\bar{6}]$	$[\bar{1},5,6]$
$[2,\bar{4},6]$	$[3,5,6]$		

Vert.Cf. 6	Ori.: 30	Freq.: $1/\tau^{3}$
$(\bar{1},3,5)$	$(\bar{1},3,6)$	
$[\bar{1},5,6]$	$[3,5,6]$	

Vert.Cf. 7	Ori.: 120		Freq.: $1/\tau^{3}$
$(\bar{1},\bar{2},5)$	$(\bar{1},3,6)$		
$[\bar{2},3,5]$	$[\bar{1},\bar{2},3]$	$[\bar{1},5,6]$	$[3,5,6]$

Vert.Cf. 8	Ori.: 120		Freq.: $1/\tau^{6}$
$(\bar{2},3,4)$	$(\bar{1},\bar{2},5)$	$(\bar{1},3,6)$	$(3,4,5)$
$[\bar{2},4,5]$	$[\bar{1},\bar{2},3]$	$[\bar{1},5,6]$	$[3,5,6]$

Vert.Cf. 9	Ori.: 60		Freq.: $2/\tau^{7}$
$(\bar{2},3,4)$	$(\bar{1},\bar{4},6)$	$(\bar{1},\bar{2},5)$	$(2,3,\bar{4})$
$(2,3,6)$	$(3,4,5)$		
$[\bar{2},4,5]$	$[\bar{1},\bar{2},3]$	$[\bar{1},3,\bar{4}]$	$[\bar{1},5,6]$
$[2,\bar{4},6]$	$[3,5,6]$		

Vert.Cf. 10	Ori.: 120		Freq.: $1/\tau^{6}$
$(\bar{2},3,4)$	$(\bar{1},\bar{4},6)$	$(\bar{1},\bar{2},5)$	$(3,4,5)$
$[\bar{2},4,5]$	$[\bar{1},\bar{2},3]$	$[\bar{1},3,\bar{4}]$	$[\bar{1},5,6]$
$[3,\bar{4},6]$	$[3,5,6]$		

Vert.Cf. 11	Ori.: 60		Freq.: $1/\tau^{3}$
$(\bar{1},\bar{4},6)$	$(\bar{1},\bar{2},5)$		
$[\bar{2},3,5]$	$[\bar{1},\bar{2},3]$	$[\bar{1},3,\bar{4}]$	$[\bar{1},5,6]$
$[3,\bar{4},6]$	$[3,5,6]$		

Vert.Cf. 12	Ori.: 60		Freq.: $2/\tau^{13}$
$(\bar{1},\bar{4},6)$	$(\bar{1},\bar{3},5)$	$(\bar{1},\bar{3},6)$	$(\bar{1},\bar{2},4)$
$(\bar{1},\bar{2},5)$	$(\bar{1},2,\bar{5})$	$(\bar{1},2,\bar{4})$	$(\bar{1},3,\bar{6})$
$(\bar{1},3,\bar{5})$	$(\bar{1},4,\bar{6})$	$(1,3,5)$	$(1,3,6)$
$(2,3,6)$	$(3,4,5)$		
$[\bar{3},5,6]$	$[\bar{2},4,5]$	$[1,5,6]$	$[2,\bar{4},6]$
$[2,3,\bar{5}]$	$[3,4,\bar{6}]$		

Vert.Cf. 13	Ori.: 120		Freq.: $2/\tau^{14}$
$(\bar{1},\bar{4},6)$	$(\bar{1},\bar{3},5)$	$(\bar{1},\bar{3},6)$	$(\bar{1},\bar{2},4)$
$(\bar{1},\bar{2},5)$	$(\bar{1},3,\bar{6})$	$(\bar{1},3,\bar{5})$	$(\bar{1},4,\bar{6})$
$(1,3,5)$	$(1,3,6)$	$(2,3,6)$	$(3,4,5)$
$[\bar{3},5,6]$	$[\bar{2},4,5]$	$[\bar{1},\bar{4},\bar{5}]$	$[1,5,6]$
$[2,\bar{4},\bar{5}]$	$[2,\bar{4},6]$	$[2,3,\bar{5}]$	$[3,4,\bar{6}]$

Vert.Cf. 14	Ori.: 30		Freq.: $(\tau^2+1)/\tau^{13}$
$(\bar{1},\bar{4},6)$	$(\bar{1},\bar{3},5)$	$(\bar{1},\bar{3},6)$	$(\bar{1},\bar{2},5)$
$(\bar{1},3,\bar{6})$	$(\bar{1},3,\bar{5})$	$(1,3,5)$	$(1,3,6)$
$(2,3,6)$	$(3,4,5)$		
$[\bar{3},5,6]$	$[\bar{2},4,\bar{6}]$	$[\bar{2},4,5]$	$[\bar{1},\bar{4},\bar{5}]$
$[1,\bar{2},\bar{6}]$	$[1,5,6]$	$[2,\bar{4},\bar{5}]$	$[2,\bar{4},6]$
$[2,3,\bar{5}]$	$[3,4,\bar{6}]$		

Vert.Cf. 15	Ori.: 60		Freq.: $1/\tau^{12}$
$(\bar{1},\bar{4},6)$	$(\bar{1},\bar{3},5)$	$(\bar{1},\bar{3},6)$	$(\bar{1},\bar{2},4)$
$(\bar{1},\bar{2},5)$	$(\bar{1},2,\bar{5})$	$(\bar{1},2,\bar{4})$	$(\bar{1},3,\bar{6})$
$(\bar{1},3,\bar{5})$	$(\bar{1},4,\bar{6})$	$(1,3,6)$	$(2,3,6)$
$[\bar{3},5,6]$	$[\bar{2},4,5]$	$[1,3,4]$	$[1,4,5]$
$[1,5,6]$	$[2,\bar{4},6]$	$[2,3,\bar{5}]$	$[3,4,\bar{6}]$

Vert.Cf. 16	Ori.: 60		Freq.: $1/\tau^{12}$
$(\bar{1},\bar{4},6)$	$(\bar{1},\bar{3},5)$	$(\bar{1},\bar{3},6)$	$(\bar{1},\bar{2},4)$
$(\bar{1},\bar{2},5)$	$(\bar{1},3,\bar{6})$	$(\bar{1},3,\bar{5})$	$(\bar{1},4,\bar{6})$
$(1,3,6)$	$(2,3,6)$		
$[\bar{3},5,6]$	$[\bar{2},4,5]$	$[\bar{1},\bar{4},\bar{5}]$	$[1,3,4]$
$[1,4,5]$	$[1,5,6]$	$[2,\bar{4},\bar{5}]$	$[2,\bar{4},6]$
$[2,3,\bar{5}]$	$[3,4,\bar{6}]$		

Vert.Cf. 17	Ori.: 120		Freq.: $2/\tau^{13}$
$(\bar{1},\bar{4},6)$	$(\bar{1},\bar{3},5)$	$(\bar{1},\bar{3},6)$	$(\bar{1},\bar{2},5)$
$(\bar{1},3,\bar{6})$	$(\bar{1},3,\bar{5})$	$(1,3,6)$	$(2,3,6)$
$[\bar{3},5,6]$	$[\bar{2},4,\bar{6}]$	$[\bar{2},4,5]$	$[\bar{1},\bar{4},\bar{5}]$
$[\bar{1},\bar{2},\bar{6}]$	$[1,3,4]$	$[1,4,5]$	$[1,5,6]$
$[2,\bar{4},\bar{5}]$	$[2,\bar{4},6]$	$[2,3,\bar{5}]$	$[3,4,\bar{6}]$

Vert.Cf. 18	Ori.: 20		Freq.: $2/\tau^{12}$
$(\bar{1},\bar{4},6)$	$(\bar{1},\bar{3},6)$	$(\bar{1},3,\bar{6})$	$(\bar{1},3,\bar{5})$
$(1,3,6)$	$(2,3,6)$		
$[\bar{3},5,6]$	$[\bar{2},\bar{3},5]$	$[\bar{2},4,\bar{6}]$	$[\bar{2},4,5]$
$[\bar{1},\bar{4},5]$	$[\bar{1},\bar{2},6]$	$[\bar{1},\bar{2},\bar{3}]$	$[1,3,4]$
$[1,4,5]$	$[1,5,6]$	$[2,\bar{4},\bar{5}]$	$[2,\bar{4},6]$
$[2,3,\bar{5}]$	$[3,4,\bar{6}]$		

Vert.Cf. 19	Ori.: 60		Freq.: $2/\tau^{14}$
$(\bar{1},\bar{4},6)$	$(\bar{1},\bar{3},5)$	$(\bar{1},\bar{3},6)$	$(\bar{1},\bar{2},5)$
$(\bar{1},3,\bar{6})$	$(\bar{1},3,\bar{5})$		
$[\bar{3},5,6]$	$[\bar{2},4,\bar{6}]$	$[\bar{2},4,5]$	$[\bar{1},\bar{4},\bar{5}]$
$[\bar{1},\bar{2},6]$	$[1,2,3]$	$[1,2,6]$	$[1,3,4]$
$[1,4,5]$	$[1,5,6]$	$[2,\bar{4},\bar{5}]$	$[2,\bar{4},6]$
$[2,3,\bar{5}]$	$[3,4,\bar{6}]$		

Vert.Cf. 20	Ori.: 30		Freq.: $1/\tau^{12}$
$(\bar{1},3,\bar{6})$	$(\bar{1},3,\bar{5})$		
$[\bar{3},4,6]$	$[\bar{3},5,6]$	$[\bar{2},\bar{3},5]$	$[\bar{2},4,\bar{6}]$
$[\bar{2},4,5]$	$[\bar{1},\bar{4},\bar{5}]$	$[\bar{1},\bar{3},4]$	$[\bar{1},\bar{2},6]$
$[\bar{1},\bar{2},\bar{3}]$	$[1,2,3]$	$[1,2,6]$	$[1,3,4]$
$[1,4,5]$	$[1,5,6]$	$[2,\bar{4},\bar{5}]$	$[2,\bar{4},6]$
$[2,3,\bar{5}]$	$[3,4,\bar{6}]$		

Vert.Cf. 21	Ori.: 60		Freq.: $2/\tau^{13}$
$(\bar{1},\bar{4},6)$	$(\bar{1},\bar{3},6)$	$(\bar{1},3,\bar{6})$	$(\bar{1},3,\bar{5})$
$[\bar{3},5,6]$	$[\bar{2},3,5]$	$[\bar{2},4,\bar{6}]$	$[\bar{2},4,5]$
$[\bar{1},4,\bar{5}]$	$[\bar{1},\bar{2},\bar{6}]$	$[\bar{1},\bar{2},\bar{3}]$	$[1,2,3]$
$[1,2,6]$	$[1,3,4]$	$[1,4,5]$	$[1,5,6]$
$[2,\bar{4},\bar{5}]$	$[2,\bar{4},6]$	$[2,3,\bar{5}]$	$[3,4,\bar{6}]$

Vert.Cf. 22	Ori.: 60		Freq.: $1/\tau^{15}$
$(\bar{1},\bar{4},6)$	$(\bar{1},\bar{3},5)$	$(\bar{1},\bar{3},6)$	$(\bar{1},\bar{2},4)$
$(\bar{1},\bar{2},5)$	$(\bar{1},3,\bar{6})$	$(\bar{1},3,\bar{5})$	$(\bar{1},4,\bar{6})$
$[\bar{3},5,6]$	$[\bar{2},4,5]$	$[\bar{1},\bar{4},\bar{5}]$	$[1,2,3]$
$[1,2,6]$	$[1,3,4]$	$[1,4,5]$	$[1,5,6]$
$[2,\bar{4},5]$	$[2,\bar{4},6]$	$[2,3,\bar{5}]$	$[3,4,\bar{6}]$

Vert.Cf. 23	Ori.: 12		Freq.: $1/\tau^{12}$
$(\bar{1},\bar{4},6)$	$(\bar{1},\bar{3},5)$	$(\bar{1},\bar{3},6)$	$(\bar{1},\bar{2},4)$
$(\bar{1},\bar{2},5)$	$(\bar{1},2,\bar{5})$	$(\bar{1},2,\bar{4})$	$(\bar{1},3,\bar{6})$
$(\bar{1},3,\bar{5})$	$(\bar{1},4,\bar{6})$		
$[\bar{3},5,6]$	$[\bar{2},4,5]$	$[1,2,3]$	$[1,2,6]$
$[1,3,4]$	$[1,4,5]$	$[1,5,6]$	$[2,\bar{4},6]$
$[2,3,\bar{5}]$	$[3,4,\bar{6}]$		

Vert.Cf. 24	Ori.: 1		Freq.: $1/\tau^{9}$
$[\bar{3},\bar{4},6]$	$[\bar{3},5,6]$	$[\bar{2},\bar{3},5]$	$[\bar{2},4,\bar{6}]$
$[\bar{2},4,5]$	$[\bar{1},\bar{5},6]$	$[\bar{1},\bar{4},\bar{5}]$	$[\bar{1},\bar{3},\bar{4}]$
$[\bar{1},\bar{2},6]$	$[\bar{1},\bar{2},\bar{3}]$	$[1,2,3]$	$[1,2,6]$
$[1,3,4]$	$[1,4,5]$	$[1,5,6]$	$[2,\bar{4},\bar{5}]$
$[2,\bar{4},6]$	$[2,3,\bar{5}]$	$[3,\bar{5},6]$	$[3,4,\bar{6}]$

Stampfli vertices that either do not contain 2's or contain the sequences 2^2,2^4,2^6, which are replaced by 4,4^2,4^3, respectively.

By omitting the rhombi in the Stampfli pattern (Baake, Klitzing & Schlottmann, 1992), we get the square-triangle pattern. It is worth mentioning because of its extreme simplicity and because it seems to be an adequate model for the dodecagonal phase of Ni-Cr. Here, $k = 2$ and $\mathcal{S} = \{3,2\}$. The pattern has altogether four vertex configurations, all mirror symmetric; only one, 3^4, is prohibited (see Fig. 8).

Finally, we quote the shield pattern (Nissen, 1990) as an example for a case where different tiles have corners with the same angles. The tiles of this pattern are an equilateral triangle *T*, a square *Sq* and a 'shield' *Sh* with equal sides *a*. The latter is a semiregular hexagon with alternating angles of $3\pi/6$ and $2\pi/6$. In order to distinguish between the right-angled corners of the square and the shield, we denote them as 3 and $\tilde{3}$, respectively. Thus, we have for the shield pattern $k = 4$ and $\mathcal{S} = \{5,3,\tilde{3},2\}$. The shield pattern can be obtained from the Gähler-Niizeki pattern by replacing all vertex configurations of the type $2^3 12^2 1 \equiv 2(12)2(21)2$ by $2\tilde{3}2\tilde{3}2 \equiv \tilde{3}2^2\tilde{3}2$. This eliminates all rhombi in the perfect pattern. Consequently, the random version of the shield pattern contains no rhombi either. There are altogether $18 + 4 = 22$ vertex configurations, which readers are urged to construct for themselves or pick out of the Stampfli list. The regular vertices are 5232, $\tilde{3}2^2\tilde{3}2$, $\tilde{3}2^2 32$, $32^2 32$.

5. The primitive icosahedral tiling

We come now to the main subject of this paper, namely the primitive icosahedral tiling - introduced independently by Kramer & Neri (1984) and Ammann (Mackay, 1981*a*,*b*; Ammann, Grünbaum & Shephard, 1992) - which is fundamental to the understanding of all known genuinely three-dimensional quasicrystalline structures. The building blocks, alias tiles or bricks, of this tiling are the well known Ammann rhombohedra (see also Kowalewski, 1938): a fat (thick, prolate or large) one L and a skinny (thin, oblate or small) one S. They have identical rhombic faces with acute angle $\alpha = \arctan 2 \simeq 63° 26' 06''$. The ratio of the large face diagonal to the small one is the golden mean $\tau = (1 + 5^{1/2})/2$. Hence, it is also easy to see that the volumes of the two rhombohedra are in a ratio of τ.

The solid angle at the acute corner around the threefold axis of the fat tile L is $\pi/5$. Thus, the solid angles spanned by its other corners are $3\pi/5$. Likewise, for the skinny tile S, the obtuse corner around the threefold axis spans a solid angle of $7\pi/5$. Hence, at the remaining corners the solid angles are again $\pi/5$. We notice that there are two different kinds of corners with the same solid angle. To distinguish between them we attach to the acute corner of L the label 1 and to that of S the label $\tilde{1}$. Thus, in our formalism we have the following. The (solid) angle unit is $\omega = 4\pi/20 = \pi/5$. The count is $s = 20$. The number of different corners is $k = 4$ and their set is $\mathcal{S} = \{7,3,\tilde{1},1\}$.

The perfect primitive icosahedral tiling contains 24 different vertex configurations, of course, up to icosahedral symmetry. Of these, eight have different enantiomers so altogether there are 32. They are listed in Table 2 and represented in Figs. 9 and 10.

Table 2 [adapted from Baake, Ben-Abraham, Kramer & Schlottmann (1990) and Ben-Abraham, Baake, Kramer & Schlottmann (1993)] shows the detailed codes of all perfect icosahedral vertices as well as their composition, symmetry multiplicity and frequency of occurrence in the ideal tiling. Fig. 9 shows these vertex configurations as constructed from the tiles represented by Schlegel diagrams. Fig. 10 shows them additionally in perspective projection. The representation of three-dimensional vertex configurations is discussed in § 6.

In the random version of the primitive icosahedral tiling there are, up to icosahedral symmetry, 5450 different vertices. Among these, 5077 have different enantiomers, so there are altogether 10 527 noncongruent

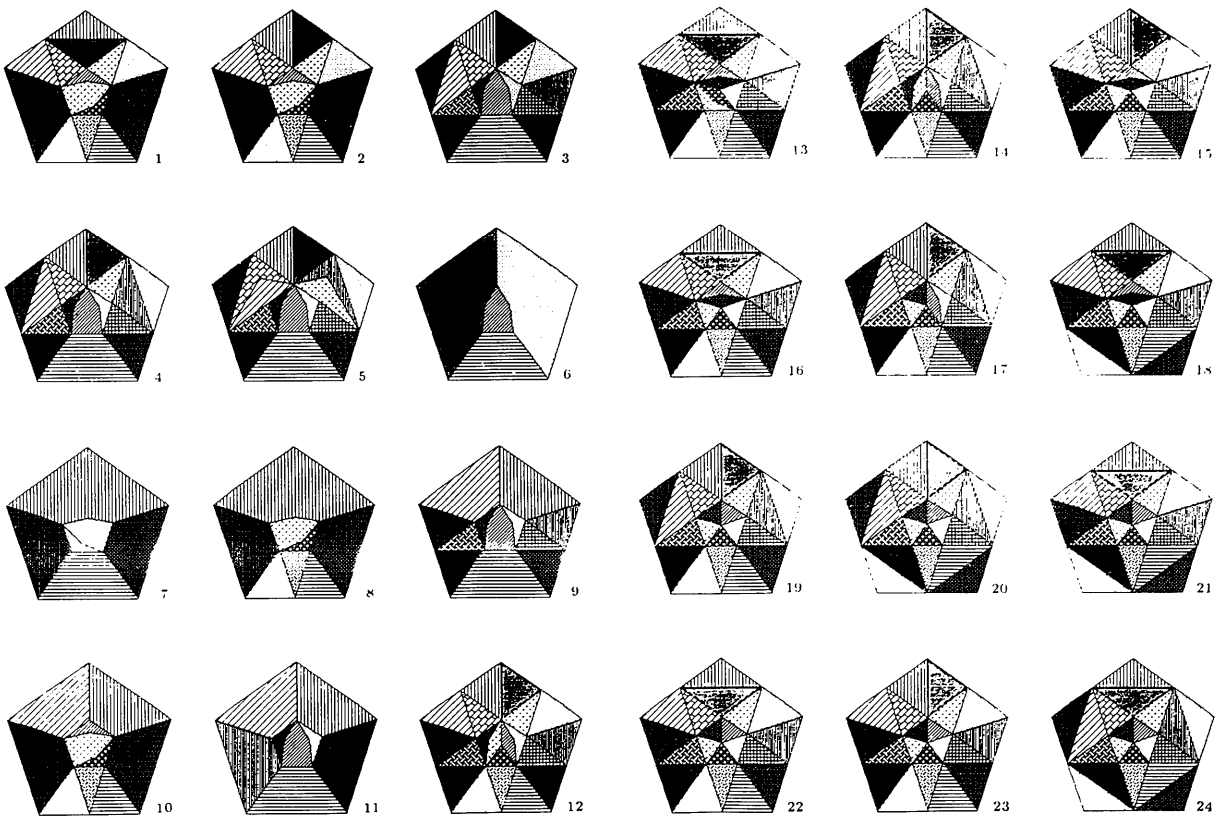

Fig. 9. The representation of the regular vertex configurations by Schlegel diagrams.

vertex configurations. Of these, 5090 (9876 if enantiomers are counted separately) are 'crystallographic', that is to say, they contain like tiles in adjacent parallel positions. Thus, there remain 360 (651) 'noncrystallographic' vertex configurations, which, of course, include the 24 (32) perfect ones.

The informal distinction between 'crystallographic' and 'noncrystallographic' vertices is quite useful, being obvious and intuitive; see also Ben-Abraham & Joseph (1993). On a formal level, it has been replaced by the classification according to rank and degree (Ben-Abraham, Baake, Kramer & Schlottmann, 1993).

It is obviously impracticable, and also useless, to present a printed list of all icosahedral vertex configurations. We therefore confine ourselves to a recapitulation, in Table 3, of the vertices according to their summary formulae.*

* Readers interested in the complete list for physical applications or any other good purpose are kindly requested to contact the authors. We will be glad to furnish the complete data in diskette form. The vertex list contains the full code, the symmetry and the multiplicity of each vertex.

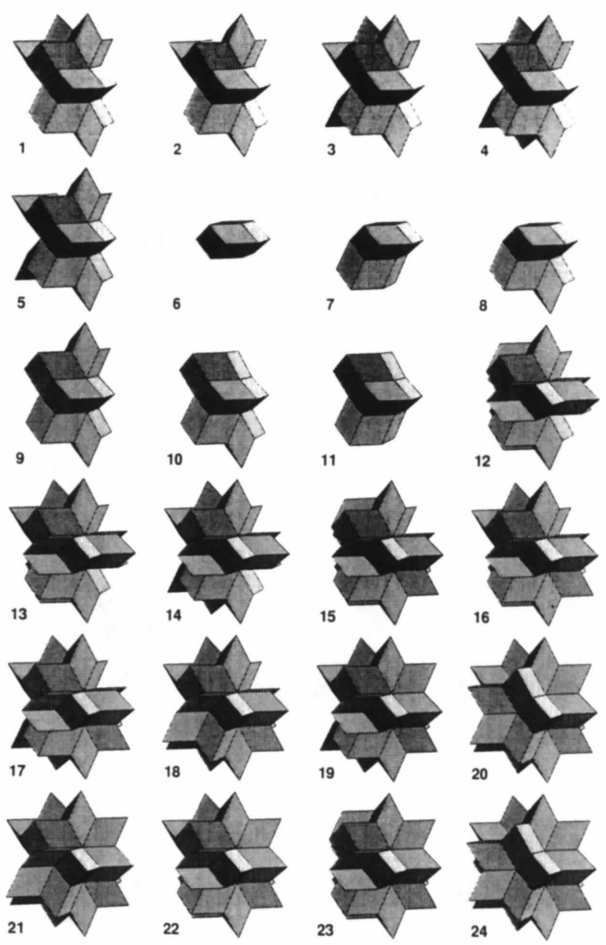

Fig. 10. The regular vertex configurations in perspective projection.

Table 3. *Number of isomeric vertex configurations of the randomized primitive icosahedral tiling within each summary partition* $\mathcal{S} = \{7,3,\bar{1},1\}$

Partition	#	Partition	#
{2,2,0,0}	1	{0,3,8,3}	353
{2,1,2,1}	1	{0,3,6,5}	221
{2,0,6,0}	2	{0,3,4,7}	43
{2,0,4,2}	1	{0,3,2,9}	3
{1,4,1,0}	2	{0,2,14,0}	11
{1,3,3,1}	9	{0,2,12,2}	207
{1,3,1,3}	1	{0,2,10,4}	595
{1,2,7,0}	5	{0,2,8,6}	510
{1,2,5,2}	21	{0,2,6,8}	177
{1,2,3,4}	5	{0,2,4,10}	29
{1,1,9,1}	11	{0,2,2,12}	2
{1,1,7,3}	22	{0,1,16,1}	18
{1,1,5,5}	10	{0,1,14,3}	199
{1,1,3,7}	1	{0,1,12,5}	544
{1,0,13,0}	1	{0,1,10,7}	581
{1,0,11,2}	8	{0,1,8,9}	300
{1,0,9,4}	16	{0,1,6,11}	81
{1,0,7,6}	10	{0,1,4,13}	11
{1,0,5,8}	3	{0,1,2,15}	1
{1,0,3,10}	1	{0,0,20,0}	2
{0,6,2,0}	5	{0,0,18,2}	18
{0,6,0,2}	2	{0,0,16,4}	103
{0,5,4,1}	31	{0,0,14,6}	252
{0,5,2,3}	8	{0,0,12,8}	325
{0,5,0,5}	1	{0,0,10,10}	228
{0,4,8,0}	21	{0,0,8,12}	103
{0,4,6,2}	144	{0,0,6,14}	30
{0,4,4,4}	62	{0,0,4,16}	7
{0,4,2,6}	6	{0,0,2,18}	1
{0,3,10,1}	83	{0,0,0,20}	1

To conclude this section, a few words are in order to explain how the vertex list was obtained. It is clearly impracticable to do a complete search of this kind by hand. At the time when this search was started, in late 1984, no computer algorithm was available. Therefore, the original search was limited to the 'noncrystallographic' vertices. Since then, one of us (MS) has invented an efficient algorithm mainly for the present purpose. The interested reader will find a detailed discussion of this algorithm in § 7.

6. Representation of three-dimensional vertex configurations

To visualize a vertex configuration, it is certainly best to have a three-dimensional model. In practice, this is, of course, impossible, except perhaps for a few basic types. We have used a two-dimensional representation of vertex configurations by means of Schlegel diagrams (Schlegel, 1883).* These are a linearization of the stereographic projection. An essentially equivalent method has been independently developed by Henley (1986).

* This old reference is not readily accessible. For those who cannot get hold of it, Grünbaum (1969) (especially chs. 3 and 11.5) is recommended; the reference has been found therein.

Let us refer to Fig. 11(*b*), which is identical with Fig. 5(*c*) of Schlegel (1883). Imagine sitting in the middle of a 20-star, that is to say, in the centre of a regular starred icosahedron. The nearest nodes one sees are the 12 vertices of a regular (simple) icosahedron. Thus, one is surrounded by 20 identical equilateral triangles. Now, place one vertex, say A, of the icosahedron on a plane so that the fivefold axis through the vertex is perpendicular to the plane. Spread the triangles upon the plane, keeping them joined along the edges. One must, of course, deform the triangles, but one can still conserve the topology and the symmetry. However, the diametrically opposite vertex A' appears on the diagram as five distinct points. Also, the edges through A', such as $A'B'$, appear twice and one must take that into account. To summarize: all triangles in the diagram (Fig. 11) are equivalent and represent the faces of a regular icosahedron. Hence, applied to a three-dimensional vertex such a triangle represents the corner 1. For clarity, different corners are distinguished by different (heraldic) colours. The choice of colours has, for the time being at least, no significance. It should be mentioned that in our diagrams some lines are drawn broken in order to show that they bisect a link between two corners.

Of course, rotating a vertex around any symmetry axis will, generally speaking, change the appearance of the diagram without changing its content. One has to be aware of that. Looking at Fig. 11, one at once recognizes that a mirror axis of the pentagon, like the straight line $A'DAD'A'$, represents a mirror plane of the icosahedron. But the broken line $BCMB'C'M'B$ (where M and M' are the midpoints of DF' and $D'F$, respectively) is equivalent to $A'DAD'A'$ and thus also represents a mirror plane. All aspects of mirror planes (up to rotations) are shown in Fig. 12.

Now, let us replace a pair of adjacent 1's by a pair of adjacent $\bar{1}$'s. Take, for instance, the 1-1 pair $\langle FBA, FBD'\rangle$. Clearly, the replacement consists of erasing the edge FB and drawing the edge AD' to create the $\bar{1}$-$\bar{1}$ pair $\langle AD'B, AD'F\rangle$. All aspects of $\bar{1}$ up to rotation are shown in Fig. 13. We leave it as an exercise for diligent readers to convince themselves (easily) that Figs. 14 and 15, respectively, show the corners 3 and 7 in their aspects.

In Henley's (1986) version, the triangles of the icosahedron are first projected onto a concentric sphere and the cap $A'B'C'D'E'F'$ is cut off and drawn separately besides the rest. Henley also shows in his diagrams the bond configuration around the vertex. That is to say, he shows the edges in the first coordination shell, as well as the short face diagonals and the short body diagonals of the thin bricks. Then he labels the vertices by their bond configurations. Unfortunately, however, it turns out that this labelling, while sufficient for his subset of vertices, is not unambiguous in general. Also, the bonds unnecessarily complicate the diagrams, and they can always be trivially reconstructed.

It is now also easy to show in the diagrams the forbidden 'crystallographic' configurations (Fig. 16).

No doubt many valid methods can be derived for coding, listing and storing the information on the configurations. We have experimented with quite a few and found it most expedient to apply the scheme of spanning vectors described in § 2. We use the double vector star $\pm e_h$ ($h = 1,\ldots,6$) abbreviated to $1,\ldots,6,\bar{1},\ldots,\bar{6}$ as shown in Fig. 11.

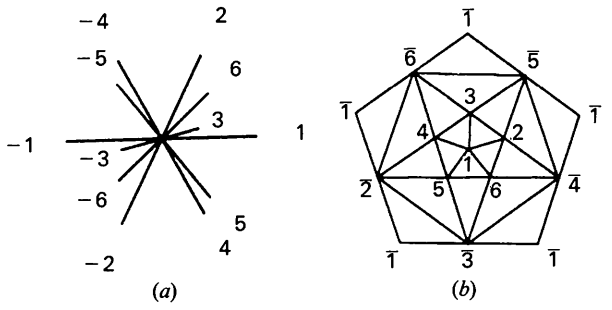

Fig. 11. Double vector star, spanning an icosahedron, and its representation as a Schlegel diagram.

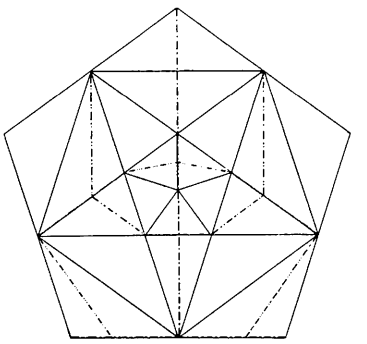

Fig. 12. Aspects of mirror planes.

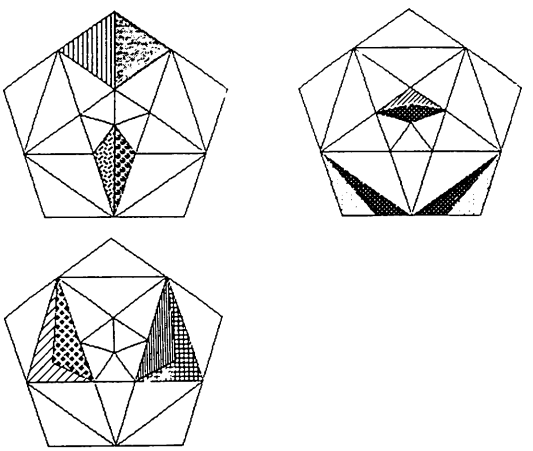

Fig. 13. Aspects of $\bar{1}$. The aspects of 1 are just the elementary triangles.

The fat tiles, L, are coded by square brackets [ ], the skinny ones, S, by round brackets ( ). Each bracket has three entries showing the vectors spanning the tile. The labels $\{7,3,\tilde{1},1\}$ of the corners entering the vertex are attached as subscripts to the bracket. Diligent readers should convince themselves that after a small amount of practice the translation between codes, Schlegel diagrams, models and even reality becomes a matter of course.

7. Search algorithm for local configurations

In the case of two-dimensional patterns, the enumeration of combinatorially possible vertex configurations can be achieved by a simple trial-and-error procedure that consists of successively adding tiles to partial vertex configurations in, for example, counterclockwise order until the full angle is completed or a mismatch occurs. Because the sphere is more complicated than the circle, things are not that simple in the case of three-dimensional patterns, *e.g.* the primitive icosahedral tiling. Here, we ran a computer program according to an algorithm that we now sketch briefly.

Seen from the central vertex of a vertex configuration, there are 160 different possible positions of the two rhombohedral tiles in question (for brevity, we speak of 160 different rhombohedra). Each of these rhombohedra occupies a certain well defined sector of the full solid angle around the central point; these sectors can be characterized as subsets of a set of 120 pairwise disjoint elementary sectors with solid angle $4\pi/120$ each (in fact, each of these elementary sectors represents a fundamental domain of the action of the icosahedral group). We enumerate the set of rhombohedra $(r_1,\ldots,r_{160})$ and the set of elementary sectors $(s_1,\ldots,s_{120})$. There is no problem in calculating a matrix of pairwise overlap between the rhombohedra and a matrix that indicates - for each rhombohedron - the set of elementary sectors it occupies; we assume in the following that these data are worked out explicitly as well as the action of the full icosahedral group on the r_i. The combinatorial problem to solve now is the calculation of a list of all sets $\{r_{i_1},\ldots,r_{i_k}\}$ with the property that every elementary sector is occupied by precisely one element r_j of them; of course, we do not want to count repeatedly such sets that are connected by an icosahedral transformation.

The algorithm proceeds recursively. In the following, P_n denotes the partial vertex configuration achieved at recursion depth n, R_n the set of rhombohedra that are candidates for being added in the next step and S_n the set of elementary sectors not covered by P_n. Furthermore, L is the list of accepted vertex configurations. Now, the following steps are carried out.

(0) Let $L = \emptyset$, $P_0 = \emptyset$, $R_0 = \{r_1,\ldots,r_{160}\}$ and $S_0 = \{s_1,\ldots,s_{120}\}$; set the recursion depth $n = 0$.

(1) If S_n is not empty, then continue with (2). Otherwise, P_n is a complete vertex configuration. Let the icosahedral group act on it and compare the results with L. If P_n turns out to be essentially new, add it to L and continue with (4).

(2) If S_n is not completely covered by the elements of R_n then continue with (4). Otherwise, increment n by 1.

(3) Choose r to be the 'minimal' element of R_{n-1} and remove it from R_{n-1}; let P_n be the join of P_{n-1} and $\{r\}$, R_n be the set of those elements of R_{n-1} that do not

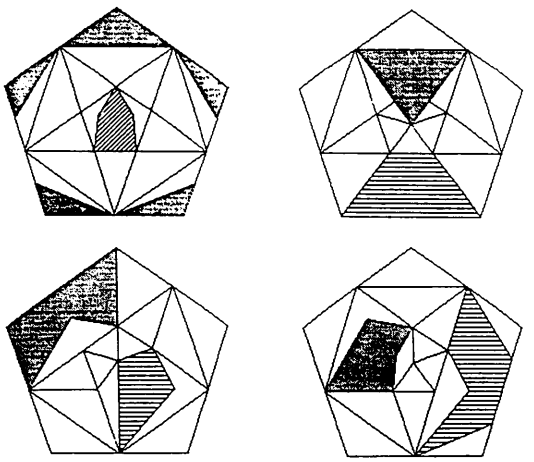

Fig. 14. Aspects of 3.

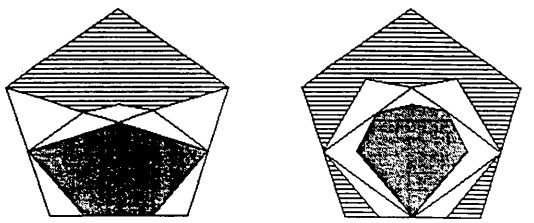

Fig. 15. Aspects of 7.

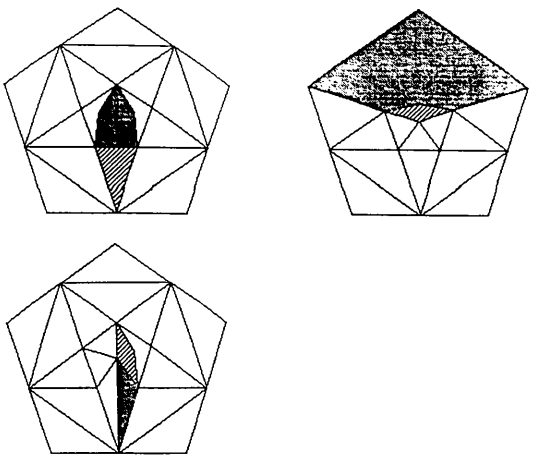

Fig. 16. Forbidden 'crystallographic' configurations.

overlap with r and S_n be the set of those elements of S_{n-1} not covered by r. Continue at (1).

(4) If $n > 0$, decrease n by 1 and continue with (1). Otherwise, terminate the calculation.

The crucial step of this procedure is (2). This bookkeeping of the possibility of covering the full angle with the remaining rhombohedra allows sufficiently early recognition of dead ends. Without this facility, it might happen that there is a large provision of rhombohedra to be added to a partial configuration while a single elementary sector is already cornered in such a way that there is no chance to cover it.

Obviously, this algorithm can be implemented in such a way that it is essentially independent of the special geometric features of the icosahedral pattern. We checked the results in the case of the triangle pattern by comparing them with the outcome of the simple-minded procedure mentioned at the beginning.

8. Formal classification of local configurations

For a generic set of tiles, out of all combinatorially possible local configurations only a small subset occurs in the corresponding perfect tiling. Hence, most configurations are defective in some sense. Intuition also tells us that some configurations are more defective than others. Clearly, a systematic classification is called for.

The defectivity of vertex configurations in quasicrystalline structures has already been dealt with from various points of view (Ben-Abraham, 1993). Here, we find it appropriate to apply the classification first introduced by Ben-Abraham, Baake, Kramer & Schlottmann (1993) and refined and extended by Ben-Abraham (1993).

A configuration that occurs in the perfect tiling is called *regular*. A configuration that does not occur in the perfect tiling is *defective*. For each configuration one can define a non-negative function μ, called the *measure of defectivity* or simply *defectivity* (Ben-Abraham, 1993). By definition, $\mu \equiv 0$ for a regular configuration. Yet it does happen that a defective configuration has vanishing defectivity. Such a configuration turns out always to be nearly perfect. We classify all configurations with $\mu = 0$ as *quasiregular*. Those of them that are not regular are called *singular*. This term was not chosen by accident. The configurations in question are indeed limiting singular cases of defectivity (Ben-Abraham, Baake, Kramer & Schlottmann, 1993). A configuration that is not quasiregular, *i.e.* one that has nonvanishing defectivity, $\mu \neq 0$, is called *prohibited*. Closer inspection of local configurations suggests a formal classification in terms of characteristic integers.

The *degree* g (for '*gradus*', say, to avoid confusion with d, often used for 'dimension') is defined only for defective vertices. It is the maximum dimension of a facet shared by such subconfigurations that does not occur in the ideal tiling. Consider, for example, the ideal primitive icosahedral tiling. A forbidden configuration of degree 2 would be one containing a pair of tiles that are translations of one another and share a face; in other words, two adjacent like tiles in parallel position. Up to now we have called such vertices 'crystallographic'. As we have seen earlier, the vast majority of the vertices in this tiling are of degree 2. Only 360 are of a lesser degree or are regular; these we have called 'noncrystallographic'. There are no configurations of degree 3 in our list; such a configuration would contain wrong tiles. One could perhaps include the regular vertices into this classification by defining their degree as -1.

We have introduced the *rank* r to distinguish between different cases of quasiregular configurations. The rank is defined as the dimension of the dual overlap. Obviously, the regular configurations are those of rank 3. It is perhaps intuitively clear that the lower the rank the more a vertex deviates from regularity. The prohibited vertices may be included into the classification by definition of their rank as -1.

Bearing in mind generalizations to more extended configurations, one is naturally led to define a third characteristic integer and call it *order*. Consider shells of tiles around some node of a tiling. These shells either are or are not complete. We confine our attention to configurations consisting of complete shells and call them, naturally, *complete configurations*. Now, the order of a complete configuration is the number of shells. More precisely, we define the order p (for '*poryadok*', say, to avoid confusion with 'origin', zero *etc.*) of a configuration around a given node as the minimum number of links leading from the node to the surface.

A vertex configuration is thus one of order 1. A point defect at a node, such as a vacancy or a foreign atom and, of course, the unperturbed node itself, becomes thus a configuration of order 0 and falls in place within our system.

We notice that the concept of a configuration of order p is related to the concept of an R map (where R is continuous) or R patch (Levitov, 1988).

9. Concluding remarks

It goes without saying that the set of local configurations present in any given structure affects its physical properties. It is important whether a local configuration appears as an isolated defect or whether it is an organic part of a more extended object. One may ask meaningful questions about spontaneous or induced formation and transformations of such objects and their consequences. The present study, being confined to local configurations of order 1, *i.e.* vertices, and focusing on the primitive icosahedral structure, is but a modest first step. Future work should include the investigation of local configura-

tions of higher order and encompass more complicated structures as well. Obviously, the extent and complexity of such research will increase quite disproportionately. Nevertheless, it is expected to be a worthwhile and rewarding undertaking.

The participation of one of us (SIBA) in this project was facilitated by the hospitality of the University of Tübingen and financial support from the Deutsche Forschungsgemeinschaft; these are gratefully acknowledged.

APPENDIX

Table 4. *Vertex configurations of the random triangular tiling*

Note that some tiles have the same angles but different edge lengths; therefore, some of the formulae are not unique and are marked by an extra *L* or *S*. This means that at this place there is a large/small edge in between.

Composition	#	Formula	Multiplicity
{2,2,0,0}	1	$3^2 2^2$	10·1
{2,1,1,1}	2	$3^2 2\bar{1}1$	10·2
{2,0,4,0}	3	$3^2 1^4$	10·1
	4	$31^2 31^2$	10·1
{2,0,2,2}	5	$3^2 1\bar{1}^2 1$	10·1
{1,3,1,0}	6	$32^3 1$	10·2
	7	$32^2 12$	10·2
{1,2,2,1}	8	$32^2 1\bar{1}1$	10·2
	9	$3212\bar{1}1$	10·2
	10	$321^2\bar{1}2$	10·2
	11	$32\bar{1}21^2$	10·2
	12	$32\bar{1}121$	10·2
	13	$312^2\bar{1}1$	10·2
{1,2,0,3}	14	$32\bar{1}^3 2$	10·1
{1,1,5,0}	15	321^5	10·2
	16	3121^4	10·2
	17	$31^2 21^3$	10·2
{1,1,3,2}	18	$321^2\bar{1}^2 1$	10·2
	19	$32\bar{1}1^2\bar{1}1$	10·2
	20	$32\bar{1}^2 1^3$	10·2
	21	$3121\bar{1}^2 1$	10·2
	22	$31^2 2\bar{1}^2 1$	10·2
	23	$31\bar{1}21\bar{1}1$	10·2
{1,1,1,4}	24	$32\bar{1}^4 1$	10·2
{1,0,6,1}	25	$31^5\bar{1}1$	10·2
	26	$31^3\bar{1}1^3$	10·1
{1,0,4,3}	27	$31^3\bar{1}^3 1$	10·2
	28	$31\bar{1}1^2\bar{1}^2 1$	10·2
{1,0,2,5}	29	$31\bar{1}^5 1$	10·1
{0,4,2,0}	30	$2^4 1^2 L$	10·1
	31	$2^4 1^2 S$	10·1
	32	$2^3 121$	10·2
	33	$2^2 12^2 1$	10·1
{0,4,0,2}	34	$2^4\bar{1}^2$	10·1
	35	$2^2\bar{1}2^2\bar{1}$	10·1
{0,3,3,1}	36	$2^3 1^3\bar{1}$	10·2
	37	$2^3 1^2\bar{1}1$	10·2
	38	$2^2 121^2\bar{1}$	10·2
	39	$2^2 121\bar{1}1$	10·2
	40	$2^2 12\bar{1}1^2$	10·2
	41	$2^2 1^2 21\bar{1}$	10·2
	42	$2^2 1^2 2\bar{1}1$	10·2
	43	$2^2 1^3 2\bar{1}$	10·2
	44	$21212\bar{1}1$	10·2
	45	$212\bar{1}21^2$	10·2
{0,3,1,3}	46	$2^3 1\bar{1}^3$	10·2
	47	$2^2 12\bar{1}^3$	10·2
	48	$2^2\bar{1}21\bar{1}^2$	10·2
	49	$2^2\bar{1}12\bar{1}^2$	10·2
{0,2,6,0}	50	$2^2 1^6 L$	10·1
	51	$2^2 1^6 S$	10·1
	52	2121^5	10·2
	53	$21^2 21^4 L$	10·1
	54	$21^2 21^4 S$	10·1
	55	$21^3 21^3$	5·2
{0,2,4,2}	56	$2^2 1^4\bar{1}^2$	10·2
	57	$2^2 1^3\bar{1}^2 1$	10·2
	58	$2^2 1^2\bar{1}1^2\bar{1}$	10·2
	59	$2^2 1^2\bar{1}^2 1^2$	10·1
	60	$2^2 1\bar{1}1^2\bar{1}1$	10·1
	61	$2^2\bar{1}1^4\bar{1}$	10·1
	62	$2121^3\bar{1}^2$	10·2
	63	$2121^2\bar{1}^2 1$	10·2
	64	$2121\bar{1}1^2\bar{1}$	10·2
	65	$21^2 21^2\bar{1}^2$	10·2
	66	$21^2 21\bar{1}^2 1$	10·1
	67	$21^2 2\bar{1}1^2\bar{1}$	10·1
	68	$21^3 21\bar{1}^2$	10·2
	69	$21^4 2\bar{1}^2$	10·1
	70	$21^3\bar{1}21\bar{1}$	10·2
	71	$21^3\bar{1}12\bar{1}$	10·2
	72	$21^2\bar{1}21\bar{1}1$	10·2
	73	$21^2\bar{1}12\bar{1}1$	10·2
{0,2,2,4}	74	$2^2 1^2\bar{1}^4$	10·2
	75	$2^2 1\bar{1}^4 1$	10·1
	76	$2^2\bar{1}1^2\bar{1}^3$	10·2
	77	$2^2\bar{1}^2 1^2\bar{1}^2$	10·1
	78	$2121\bar{1}^4$	10·2
	79	$21^2 2\bar{1}^4$	10·1
	80	$21\bar{1}21\bar{1}^3$	10·2
	81	$21\bar{1}12\bar{1}^3$	10·1
	82	$21\bar{1}^2 21\bar{1}^2$	5·2
	83	$21\bar{1}^2 12\bar{1}^2$	10·1
	84	$21\bar{1}^3 12\bar{1}$	10·1
{0,2,0,6}	85	$2^2\bar{1}^6$	10·1
{0,1,7,1}	86	$21^7\bar{1}$	10·2
	87	$21^6\bar{1}1$	10·2
	88	$21^5\bar{1}1^2$	10·2
	89	$21^4\bar{1}1^3$	10·2
{0,1,5,3}	90	$21^5\bar{1}^3$	10·2
	91	$21^4\bar{1}^3 1$	10·2
	92	$21^3\bar{1}1^2\bar{1}^2$	10·2
	93	$21^3\bar{1}^2 1^2\bar{1}$	10·2
	94	$21^3\bar{1}^3 1^2$	10·2
	95	$21^2\bar{1}1^2\bar{1}^2 1$	10·2
	96	$21^2\bar{1}^2 1^2\bar{1}1$	10·2
	97	$21\bar{1}1^4\bar{1}^2$	10·2
	98	$21\bar{1}1^2\bar{1}1^2\bar{1}$	10·2
	99	$21\bar{1}^2 1^4\bar{1}$	10·2
{0,1,3,5}	100	$21^3\bar{1}^5$	10·2
	101	$21^2\bar{1}^5 1$	10·2
	102	$21\bar{1}1^2\bar{1}^4$	10·2
	103	$21\bar{1}^2 1^2\bar{1}^3$	10·2
	104	$21\bar{1}^3 1^2\bar{1}^2$	10·2
	105	$21\bar{1}^4 1^2\bar{1}$	10·2
{0,1,1,7}	106	$21\bar{1}^7$	10·2
{0,0,10,0}	107	1^{10}	2·1
{0,0,8,2}	108	$1^8\bar{1}^2$	10·1
	109	$1^6\bar{1}1^2\bar{1}$	10·1
	110	$1^4\bar{1}1^4\bar{1}$	5·1
{0,0,6,4}	111	$1^6\bar{1}^4$	10·1
	112	$1^4\bar{1}1^2\bar{1}^3$	10·2
	113	$1^4\bar{1}^2 1^2\bar{1}^2$	10·1
	114	$1^2\bar{1}1^2\bar{1}1^2\bar{1}^2$	10·1
{0,0,4,6}	115	$1^4\bar{1}^6$	10·1
	116	$1^2\bar{1}1^2\bar{1}^5$	10·1
	117	$1^2\bar{1}^2 1^2\bar{1}^4$	10·1
	118	$1^2\bar{1}^3 1^2\bar{1}^3$	5·1
{0,0,2,8}	119	$1^2\bar{1}^8$	10·1
{0,0,0,10}	120	$\bar{1}^{10}$	1·1

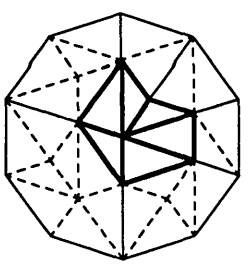

Fig. 17. One representative vertex figure. It shows in addition that they are all embeddable into the perfect triangular tiling. The decagons are allowed patches. The edges of the vertex configuration define sectors inside the decagon and it is shown how they can be filled up.

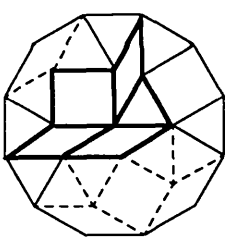

Fig. 18. One representative vertex figure. It shows in addition that they are all embeddable into the perfect Stampfli tiling. The dodecagons are allowed patches. The edges of the vertex configuration define sectors inside the dodecagon and it is shown how they can be filled up.

Table 5. *Vertex configurations of the random Stampfli tiling*

Composition	#	Formula	Multiplicity
{2,0,1,0}	1	$5^2 2$	12·1
{2,0,0,2}	2	$5^2 1^2$	12·1
	3	5151	6·1
{1,2,0,1}	4	$53^2 1$	12·2
	5	5313	12·1
{1,1,2,0}	6	532^2	12·2
	7	5232	12·1
{1,1,1,2}	8	5321^2	12·2
	9	53121	12·2
	10	$531^2 2$	12·2
	11	5231^2	12·2
	12	52131	12·2
	13	51321	12·2
{1,1,0,4}	14	531^4	12·2
	15	5131^3	12·2
	16	$51^2 31^2$	12·1
{1,0,3,1}	17	$52^3 1$	12·1
	18	$52^2 12$	12·2
{1,0,2,3}	19	$52^2 1^3$	12·2
	20	52121^2	12·2
	21	$521^2 21$	12·2
	22	$521^3 2$	12·1
	23	$512^2 1^2$	12·2
	24	512121	12·1
{1,0,1,5}	25	521^5	12·2
	26	5121^4	12·2
	27	$51^2 21^3$	12·2
{1,0,0,7}	28	51^7	12·1
{0,4,0,0}	29	3^4	3·1
{0,3,1,1}	30	$3^3 21$	12·2
	31	$3^2 231$	12·2
{0,3,0,3}	32	$3^3 1^3$	12·1
	33	$3^2 131^2$	12·2
	34	313131	4·1
{0,2,3,0}	35	$3^2 2^3$	12·1
	36	3232^2	12·1
{0,2,2,2}	37	$3^2 2^2 1^2$	12·2
	38	$3^2 2121$	12·2
	39	$3^2 2112$	12·1
	40	$3^2 1221$	12·1
	41	32321^2	12·2
	42	323121	12·1
	43	$32^2 31^2$	12·1
	44	$32^2 131$	12·2
	45	321321	12·2
	46	321312	12·1
	47	321231	12·1
{0,2,1,4}	48	$3^2 21^4$	12·2
	49	$3^2 121^3$	12·2
	50	$3^2 1^2 21^2$	12·1
	51	3231^4	12·1
	52	32131^3	12·2
	53	$321^2 31^2$	12·2
	54	$321^3 31$	12·2
	55	$3121^2 31$	12·2
	56	312131^2	12·1
{0,2,0,6}	57	$3^2 1^6$	12·1
	58	3131^5	12·1
	59	$31^2 31^4$	12·1
	60	$31^3 31^3$	6·1
{0,1,4,1}	61	$32^4 1$	12·2
	62	$32^3 12$	12·2
	63	$32^2 12^2$	12·1
{0,1,3,3}	64	$32^3 1^3$	12·2
	65	$32^2 121^2$	12·2
	66	$32^2 1^2 21$	12·2
	67	$32^2 1^3 2$	12·2
	68	$3212^2 1^2$	12·2
	69	3212121	12·2
	70	$32121^2 2$	12·2
	71	$321^2 2^2 1$	12·2
	72	$312^3 1^2$	12·2
	73	$312^2 121$	12·2
{0,1,2,5}	74	$32^2 1^5$	12·2
	75	32121^4	12·2
	76	$321^2 21^3$	12·2
	77	$321^3 21^2$	12·2
	78	$321^4 21$	12·2
	79	$321^5 2$	12·1
	80	$312^2 1^4$	12·2
	81	312121^3	12·2
	82	$3121^2 21^2$	12·2
	83	$3121^3 21$	12·1
	84	$31^2 2^2 1^3$	12·2
	85	$31^2 2121^2$	12·1
{0,1,1,7}	86	321^7	12·2
	87	3121^6	12·2
	88	$31^2 21^5$	12·2
	89	$31^3 21^4$	12·2
{0,1,0,9}	90	31^9	12·1
{0,0,6,0}	91	2^6	2·1
{0,0,5,2}	92	$2^5 1^2$	12·1
	93	$2^4 121$	12·1
	94	$2^3 12^2 1$	12·1
{0,0,4,4}	95	$2^4 1^4$	12·1
	96	$2^3 121^3$	12·2
	97	$2^3 1^2 21^2$	12·1
	98	$2^2 12^2 1^3$	12·1
	99	$2^2 12121^2$	12·2
	100	$2^2 121^2 21$	12·1
	101	$2^2 1^2 2^2 1^2$	6·1
	102	21212121	3·1
{0,0,3,6}	103	$2^3 1^6$	12·1
	104	$2^2 121^5$	12·2
	105	$2^2 1^2 21^4$	12·2
	106	$2^2 1^3 21^3$	12·1
	107	212121^4	12·1
	108	$2121^2 21^3$	12·2
	109	$21^2 21^2 21^2$	4·1
{0,0,2,8}	110	$2^2 1^8$	12·1
	111	2121^7	12·1
	112	$21^2 21^6$	12·1
	113	$21^3 21^5$	12·1
	114	$21^4 21^4$	6·1
{0,0,1,10}	115	21^{10}	12·1
{0,0,0,12}	116	1^{12}	1·1

References

Ammann, R., Grünbaum, B. & Shephard, G. C. (1992). *Discr. Comput. Geom.* **8**, 1-25.

Baake, M., Ben-Abraham, S. I., Kramer, P. & Schlottmann, M. (1990). *Quasicrystals and Incommensurate Structures in Condensed Matter*, edited by M. J. Yacamán, D. Romeu, V. Castaño & A. Gómez, pp. 85-89. Singapore: World Scientific.

Baake, M. & Joseph, D. (1990). *Phys. Rev. B*, **42**, 8091-8102.

Baake, M., Klitzing, R. & Schlottmann, M. (1992). *Physica (Utrecht)*, **A191**, 554-558.

Baake, M., Kramer, P., Schlottmann, M. & Zeidler, D. (1990*a*). *Mod. Phys. Lett. B*, **4**, 249-258.

Baake, M., Kramer, P., Schlottmann, M. & Zeidler, D. (1990*b*). *Int. J. Mod. Phys. B*, **4**, 2217-2268.

Baake, M., Kramer, P., Schlottmann, M. & Zeidler, D. (1990*c*). *Quasicrystals, Networks, and Molecules of Fivefold Symmetry*, edited by I. Hargittai, ch. 9. New York: VCH.

Baake, M., Schlottmann, M. & Jarvis, P. D. (1991). *J. Phys. A: Gen. Phys.* **24**, 4637-4654.

Bancel, P. A. (1991). *Quasicrystals: the State of the Art*, pp. 17-55, edited by D. P. DiVicenzo & P. J. Steinhardt. Singapore: World Scientific.

Becker, R. S. & Kortan, A. R. (1991). *Quasicrystals: the State of the Art*, pp. 111-132, edited by D. P. DiVicenzo & P. J. Steinhardt. Singapore: World Scientific.

Ben-Abraham, S. I. (1993). *Int. J. Mod. Phys. B*, **7**, 1415-1425.

Ben-Abraham, S. I., Baake, M., Kramer, P. & Schlottmann, M. (1993). *J. Non-Cryst. Solids*, **153&154**, 132-136.

Ben-Abraham, S. I. & Joseph, A. (1993). *Phase Transit.* **44**, 51-57.

DiVicenzo, D. P. & Steinhardt, P. J. (1991). *Quasicrystals: the State of the Art*, edited by D. P. DiVicenzo & P. J. Steinhardt, pp. 1-16. Singapore: World Scientific.

Duneau, M. & Katz, A. (1985). *Phys. Rev. Lett.* **54**, 2688-2691.

Elser, V. (1985). *Phys. Rev. Lett.* **54**, 1730.

Gähler, F. (1988). *Quasicrystalline Materials*, edited by C. Janot & J. M. Dubois, p. 272. Singapore: World Scientific.

Gardner, M. (1977). *Sci. Am.* **236**, 110-121.

Grünbaum, B. (1969). *Convex Polytopes*, pp. 42*ff*. London: Wiley.

Grünbaum, B. & Shephard, G. C. (1987). *Tilings and Patterns*. New York: Freeman.

Hardy, H. K. & Silcock, J. (1955/56). *J. Inst. Met.* **24**, 423.

Henley, C. L. (1986). *Phys. Rev. B*, **34**, 797-816.

Henley, C. L. (1990). *Quasicrystals and Incommensurate Structures in Condensed Matter*, edited by M. J. Yacamán, D. Romeu, V. Castaño & A. Gómez, pp. 152-169. Singapore: World Scientific.

Henley, C. L. (1991). *Quasicrystals: the State of the Art*, edited by D. P. DiVicenzo & P. J. Steinhardt, pp. 429-524. Singapore: World Scientific.

HIRAGA, K. (1991). *Quasicrystals: the State of the Art*, edited by D. P. DIVICENZO & P. J. STEINHARDT, pp. 95-110. Singapore: World Scientific.
ISHIMASA, T., NISSEN, H.-U. & FUKANO, Y. (1984). Workshop on Physics of Small Particles, Gwatt, Switzerland, October 1984.
JARIĆ, M. V. (1990). *Period. Mineral.* **59**, 11-29.
KATZ, A. & DUNEAU, M. (1986). *J. Phys. (Paris)*, **47**, C3, 103-112.
KLITZING, R. (1992). Thesis, Univ. Tübingen, Germany.
KORTAN, A. R., BECKER, R. S., THIEL, F. A. & CHEN, H. S. (1990). *Phys. Rev. Lett.* **64**, 200-203.
KOWALEWSKI, G. (1938). *Der Keplersche Körper und andere mathematische Bauspiele*. Leipzig: Kohlers Antiq.
KRAMER, P. & NERI, R. (1984). *Acta Cryst.* A**40**, 580-587.
LEVINE, D. & STEINHARDT, P. J. (1984). *Phys. Rev. Lett.* **53**, 2477-2480.
LEVINE, D. & STEINHARDT, P. J. (1986). *Phys. Rev. B.* **34**, 596-616.
LEVITOV, L. S. (1988). *Commun. Math. Phys.* **119**, 627-666.
MACKAY, A. L. (1981*a*). *Kristallografiya*, **26**, 910-919.
MACKAY, A. L. (1981*b*). *Sov. Phys. Crystallogr.* **26**, 517-522.
NIIZEKI, K. & MITANI, H. (1987). *J. Phys. A: Gen. Phys.* **20**, L405-L410.
NISSEN, H.-U. (1990). *Quasicrystals, Networks, and Molecules of Fivefold Symmetry*, edited by I. HARGITTAI, ch. 11, pp. 181-199. New York: VCH.
NISSEN, H.-U. & BEELI, C. (1990). *Period. Mineral.* **59**, 31-67.
NISSEN, H.-U. & BEELI, C. (1993). *Int. J. Mod. Phys. B*, **7**, 1387-1413.
PAULING, L. (1985). *Nature (London)*, **317**, 512-514.
ROBINSON, R.M. (1975). *Comments on Penrose Tiles*. Berkeley: Univ. of California.
SASTRY, G. V. S., SURYANARAYANA, C., VAN SANDE, M. & VAN TENDELOO, G. (1978). *Mater. Res. Bull.* **13**, 1065.
SCHLEGEL, V. (1883). *Nova Acta Acad. Caesareae Leopold.-Carolin. Ger. Naturae Curiosorum*, **44**, 337-459. (Full journal: *Verhandlungen der Kaiserlichen Leopoldinisch-Carolinischen Deutschen Akademie der Naturforscher*, Halle, Germany.)
SHECHTMAN, D., BLECH, I., GRATIAS, D. & CAHN, J. W. (1984). *Phys. Rev. Lett.* **53**, 1951-1953.
SOCOLAR, J. E. S. (1989). *Phys. Rev. B*, **39**, 10519-10551.
SOCOLAR, J. E. S. & STEINHARDT, P. J. (1986). *Phys. Rev. B*, **34**, 617-647.
STAMPFLI, P. (1990). *Quasicrystals, Networks, and Molecules of Fivefold Symmetry*, edited by I. HARGITTAI, ch. 11, pp. 201-221. New York: VCH.
STEURER, W. & KUO, K. H. (1990). *Philos. Mag. Lett.* **62**, 175-182.
TANG, L.-H. (1990). *Period. Mineral.* **59**, 101-114.
WIDOM, M., STRANDBURG, K. J. & SWENDSEN, R. H. (1987). *Phys. Rev. Lett.* **58**, 706-709.

Acta Cryst. (1994). A**50**, 566–574

Convergent-Beam Electron Diffraction Study of Incommensurately Modulated Crystals. II. (3 + 1)-Dimensional Space Groups

BY MASAMI TERAUCHI, MARIKO TAKAHASHI* AND MICHIYOSHI TANAKA

Research Institute for Scientific Measurements, Tohoku University, Sendai 980, *Japan*

(*Received* 2 *July* 1993; *accepted* 20 *September* 1993)

Abstract

The convergent-beam electron diffraction (CBED) method for determining three-dimensional space groups is extended to the determination of the (3 + 1)-dimensional space groups for one-dimensional incommensurately modulated crystals. It is clarified than an approximate dynamical extinction line appears in the CBED discs of the reflections caused by an incommensurate modulation. The extinction enables the space-group determination of the (3 + 1)-dimensional crystals or the one-dimensional incommensurately modulated crystals. An example of the dynamical extinction line is shown using an incommensurately modulated crystal of $Sr_2Nb_2O_7$. Tables of the dynamical extinction lines appearing in CBED patterns are given for all the (3 + 1)-dimensional space groups of the incommensurately modulated crystal.

1. Introduction

The space groups of three-dimensional crystals can be determined by the convergent-beam electron diffraction (CBED) method. The method is based on dynamical extinction, which permits an unambiguous identification of 2_1 screw axes and glide planes. The dynamical extinction effect in electron diffraction at a symmetrical incidence was discussed theoretically by Cowley & Moodie (1959), Miyake, Takagi & Fujimoto (1960) and Cowley, Moodie, Miyake, Takagi & Fujimoto (1961). Goodman & Lehmpfuhl (1964) first observed the dynamical extinction as dark cross bands or lines in kine-

* Present address: NEC Corporation, Minamihashimoto 3-1-35, Sagamihara, Kanagawa 229, Japan.